

Ferromagnet-semiconductor nanowire coaxial heterostructures grown by molecular-beam epitaxy

M. Hilse,^{a)} Y. Takagaki, J. Herfort, M. Ramsteiner, C. Herrmann, S. Breuer, L. Geelhaar, and H. Riechert

Paul-Drude-Institut für Festkörperelektronik, Hausvogteiplatz 5–7, 10117 Berlin, Germany

(Received 28 July 2009; accepted 9 September 2009; published online 2 October 2009)

GaAs–MnAs core-shell structures are grown by molecular-beam epitaxy using wurtzite GaAs nanowires on GaAs(111)*B*. The nanowire structures curve due to the strain at the heterointerface when the substrate is not rotated during the growth, evidencing the diffusion length in the MnAs overgrowth being less than the perimeter of the columns. The MnAs growth is thus demonstrated to take place by direct deposition on the sidewall. The MnAs envelope is *m*-plane-oriented with the *c*-axis along the nanowire axis. The magnetic easy axis hence lies in the surface plane of the substrate, which is confirmed by magnetization measurements and magnetic-force microscopy.

© 2009 American Institute of Physics. [doi:10.1063/1.3240405]

Nanowires synthesized by a self-organized crystal growth are promising as a building block for nanoscale devices. As the nanowires can elastically absorb lattice-mismatch strain, they can grow not only on dissimilar substrates but also as axial and radial heterostructures in high qualities.¹ Such capabilities allow realization of the entire device structure by only a sequence of growths and distinguish the nanowires from planar films and nanodots.

When a ferromagnet is incorporated in nanowires, spin-dependent functionalities can be introduced to nanowire devices. (A single-photon source with a defined circular polarization is an example.) MnAs is one of the attractive materials for spintronics applications as the Curie temperature (about 40 °C) is above room temperature. MnAs can be grown epitaxially on GaAs.² Spin injection from a MnAs layer to a GaAs–(In,Ga)As quantum well in planar heterostructures has already been demonstrated.³ In addition, ferromagnetic nanotubes, for instance, are intriguing as their magnetic textures experience geometrical constraints.⁴

In this study, we realized ferromagnet-semiconductor structures by growing MnAs layers to wrap wurtzite GaAs nanowires. In contrast to previously reported core-shell structures, in which similar materials were combined,¹ the growth of the GaAs–MnAs heterostructures could face obstacles as the lattice mismatch is large. (The crystal structure of MnAs is hexagonal.) We evidence that the MnAs growth takes place by direct deposition on the sidewall of nanowires. To identify the epitaxial orientation relationship in the coaxial heterostructure as well as the direction of the magnetic easy axis, we evaluate the nanowire geometry and the magnetic properties.

Nanowires were grown based on the vapor-liquid-solid mechanism.¹ The growth was carried out by molecular-beam epitaxy (MBE) on GaAs(111)*B* substrates. We grew a GaAs buffer layer at 600 °C with an As₄/Ga beam equivalent pressure (BEP) ratio of 46 and a growth rate of 220 nm/h. The reflection high-energy electron diffraction (RHEED) pattern changed from a ($\sqrt{19} \times \sqrt{19}$) reconstruction after the buffer layer growth to a (2 × 2) structure during cooling to

400 °C. A 0.6-nm-thick Au layer was then deposited for a catalyst. To force the Au layer to form droplets, we annealed the substrate for 5 min at 550 °C. The growth of GaAs nanowires having an average diameter of 26 nm was carried out at 500 °C with an As₄/Ga BEP ratio of 35 and a growth rate of 400 nm/h. The nanowires were about 1.7 μm long. The crystal structure of Au-induced GaAs nanowires is known to be wurtzite,⁵ which was indeed observed by RHEED. Due to the small diameter, RHEED exhibited patterns associated with transmission across the nanowires. High-symmetry directions [0001], [01 $\bar{1}$ 0], and [$\bar{2}$ 110] of the nanowires were found to be parallel to the [111], [$\bar{2}$ 11], and [01 $\bar{1}$] directions of the substrate, respectively. Finally, MnAs growth took place using the typical conditions for planar growth on GaAs,² i.e., at 250 °C with an As₄/Mn BEP ratio of 330 and a growth rate of 30 nm/h.

In Figs. 1(a)–1(c), we show scanning-electron micrographs of three samples. The duration of the MnAs growth for samples A and B was such that the planar layers on the substrates were 60- and 240-nm-thick, respectively. While the sample stage was rotated during the growth of these

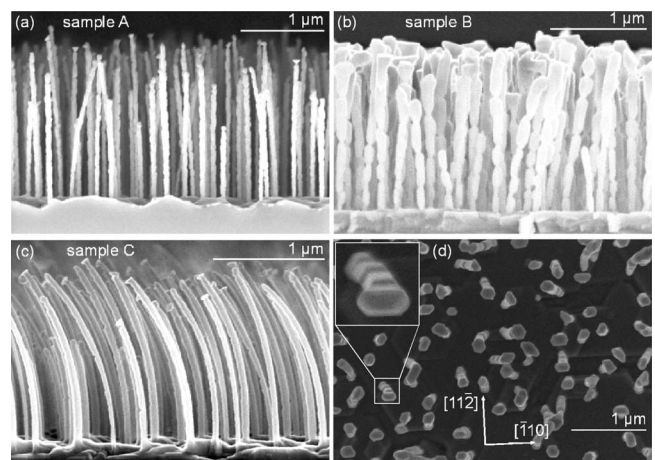


FIG. 1. Scanning electron micrographs of GaAs nanowires enveloped by MnAs on GaAs(111)*B*. The substrate was rotated during growth for [(a) and (b)], whereas it was not for (c). A plane view of sample B is shown in (d). The [$\bar{1}$ 10] and [$\bar{2}$ 11] directions of the substrate are indicated. The inset shows an individual nanowire with expanded scales.

^{a)}Electronic mail: wagler@pdi-berlin.de.

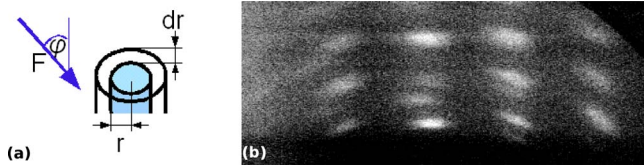


FIG. 2. (Color online) (a) Radial growth of a nanowire having a radius of r . The flux impinging at a rate of F is inclined by an angle of φ . (b) RHEED pattern in the $[\bar{1}10]$ azimuth of sample C. The image was taken at the growth temperature after the MnAs overgrowth.

samples, it was not rotated for sample C (corresponding layer thickness was 60 nm). One finds that the MnAs shells roughened. The morphological instability was driven by the large lattice mismatch,⁶ which we will discuss elsewhere.

The nanowires in samples A and B are straight and perpendicular to the surface. In contrast, those in sample C are uniformly curved. As illustrated in Fig. 2(a), the impinging fluxes are inclined with respect to the substrate normal in a MBE system. Thus, the amount of Mn atoms arriving to the regions of the nanowires facing and opposite to the cell differs if the stage is not rotated. This led to different shell thicknesses in the two regions. (Note that the growth was performed under As-rich conditions.) The asymmetric shell thickness gives rise to an imbalance of the stresses at the GaAs–MnAs interfaces, resulting in the bending.

The shell thicknesses in the present study are more than one order of magnitude larger than the critical thickness for coherent growth of MnAs layers on GaAs.⁷ The lattice mismatch is hence compensated by the introduction of misfit dislocations during growth. Nevertheless, the heterointerface is strained at room temperature as the thermal expansion mismatch is significant. [This implies that the MnAs shell is thicker at the left-hand side than at the right-hand side in Fig. 1(c).] As we will discuss later, the c -axis of MnAs is aligned along the axis of the nanowires. The total mismatch is thus estimated to be $\varepsilon = 1.6\%$.⁸ While there is no theory available for the off-centered core-shell structure, the curvature radius R of the bending of a bilayer system is related to ε as⁹

$$R = (h_1 + h_2)^3 / (6\varepsilon h_1 h_2), \quad (1)$$

where h_1 and h_2 are the thicknesses of the two layers. The bending is maximal when $h_1 = h_2$, where $R = 1.9 \mu\text{m}$ if we set the diameter of the GaAs core for h_1 . The experimental value $R \approx 2.6 \mu\text{m}$ in sample C is thus reasonable.

To be precise, the relaxation of the stress in the MnAs shell during the growth is not complete. The tiny bending of the nanowires (at growth temperature) resulting from the residual stress was detected for sample C as a ring-shaped RHEED pattern, as shown in Fig. 2(b). (The pattern was a rectangular grid before MnAs overgrowth.)

The length L of the nanowires remained almost unchanged during the MnAs growth. The asymmetry in Fig. 1(c) indicates that the diffusion length of the Mn adatoms is shorter than the perimeter (about 160 nm) of the nanowires. Therefore, the catalyst was practically inactive and the envelope grew by adsorption on the nanowire sidewalls. The growth on the sidewall is slower than that on the surface of the substrate due to a geometrical effect.¹⁰ The material supplied by the flux to the sidewall during a time interval dt contributes to the increase of the nanowire radius r . We thus obtain $(2r)(L \sin \varphi)Fdt = (2\pi r dr)L$, where φ and F are the incidence angle and the flux rate, respectively. As the rate of

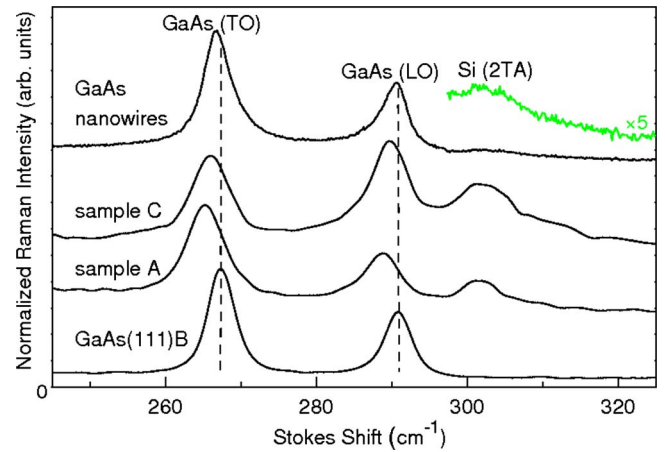


FIG. 3. (Color online) Raman spectra at room temperature from samples A and C, GaAs nanowires, and a GaAs(111)B substrate. The nanowires were placed on SiO₂/Si substrates. The peaks are associated with the LO and TO phonons in GaAs and the transverse acoustic (TA) phonons (second order) in Si. Curves are offset for clarity.

the radius increase is $dr/dt = F \sin \varphi / \pi$, the thickness h_{env} of the envelope layer is related to the thickness h_f of the film on the substrate as $h_{\text{env}} = (\tan \varphi / \pi)h_f$. For our growth chamber, we expect $h_{\text{env}} = 0.2h_f$ as $\varphi \approx 30^\circ$. The diameters of the nanowires were 52 nm for samples A and C. We thus indeed find $h_{\text{env}} = 0.2h_f$ experimentally.

The nanowire diameter in sample B increased from about 68 nm at the base to about 155 nm at the top. This tapered shape is due to the shadowing of nanowires from the incoming flux by those in front of them. The nanowires grew uniformly up to a diameter of ~ 68 nm as they were sparsely distributed. As the diameter further increased, the flux could no longer reach the base of the nanowires, resulting in the conical shape of the columns. The critical diameter for shadowing is roughly given by $(\rho L \sin \varphi)^{-1} = 84$ nm.¹¹ Here, $\rho = 14.7 \mu\text{m}^{-2}$ is the areal density of the nanowires. The top being broader than the base is another evidence for the negligible diffusion of Mn adatoms along the nanowires.

A long diffusion along the nanowires is generally considered to be essential for the growth and the adsorption at the sidewalls is often ignored, i.e., φ is assumed to be zero.¹² The growth of MnAs shells without diffusion evidences that the deposition to the sidewalls is, in fact, considerable.¹³ The ratio of the amounts of adatoms supplied by the direct deposition on the sidewalls ($2rL \sin \varphi F$) and on the substrate ($\rho^{-1}F \cos \varphi$) is $2r\rho L \tan \varphi$, which equals, for instance, 0.4 for $L = 1.7 \mu\text{m}$ and $r = 13$ nm.

In Fig. 3, we compare the Raman spectra from samples A and C with those from GaAs nanowires and a GaAs(111)B substrate. Due to the thick MnAs shell, the Raman signal was undetectable in sample B. The nanowires were placed on Si substrates covered by SiO₂. The peaks associated with the longitudinal optic (LO) and transverse optic (TO) phonons in GaAs are shifted to lower frequencies in the nanowires in comparison to those in the substrate. The shift in the uncovered GaAs nanowires is due to the wurtzite structure of GaAs (Ref. 14) and the size effect.¹⁵ The large additional shift in the MnAs-overgrown nanowires is attributed to the strain imposed by the overlayer. The strain is indicated to be inhomogeneous as the peaks are broadened.

The epitaxial orientation relationship between the envelope and the core is determined by the minimization of the

TABLE I. Ratio $u_{\text{GaAs}}/u_{\text{MnAs}}$ of the surface-unit-cell lengths of wurtzite GaAs and MnAs planes in the direction orthogonal to the c -axis at the growth temperature. The c -axes of GaAs and MnAs are assumed to be parallel to each other. The lattice parameters for GaAs and MnAs have been taken from Refs. 20 and 8, respectively.

	GaAs(1 $\bar{1}00$)	GaAs(11 $\bar{2}0$)
MnAs(1 $\bar{1}00$)	1.07	1.86
MnAs(11 $\bar{2}0$)	0.62	1.07

strain and bonding energies. In Fig. 1(d), we show a top view of sample B. As shown in the inset, the cross section of the nanowires has a hexagonal shape even when the outer diameter of the shell is much larger than the diameter of the core, indicating that the c -axis of MnAs in the envelope is oriented to be parallel to the nanowire axis. Ramlan *et al.*¹⁶ reported a growth of self-assembled MnAs nanodots on the sidewalls of wurtzite InAs nanowires on Si(001). The c -axis was also found to be aligned along the nanowire axis.

The matching between the participating lattices in the direction orthogonal to the c -axis is summarized in Table I. As the crystal structures of both the core and the shell are hexagonal, we consider the cases of nanowire sidewalls being composed of either m - or a -planes. From the viewpoint of the strain energy, MnAs layers are anticipated to grow with the m - and a -plane orientations when the GaAs sidewall exhibits m - and a -plane facets, respectively. Such an epitaxial orientation relationship having identical surface orientations would be favorable also in terms of the bonding energy.

The sidewall facets of the GaAs–MnAs nanowires are perpendicular to the $\langle\bar{2}11\rangle$ directions of the substrate, and so they consist of m -planes. The lattice mismatch in the c -axis direction is $c_{\text{GaAs}}/c_{\text{MnAs}}=1.13\approx 7/6$.¹⁷ The mismatch is hence anticipated to be accommodated by the coincidence lattice.¹⁸ We note that the ratio becomes 0.99 if the MnAs shell is (1 $\bar{1}01$)-oriented. Thus, we cannot rule out the possibility that the envelope layers are (1 $\bar{1}01$)-oriented.

For other growth approaches, the formation of zinc blende GaAs nanowires has been observed.¹⁹ For such a GaAs core, the c -axis orientation in the MnAs shell would be altered. The side surface of cubic GaAs nanowires grown in the [111] direction is likely to consist of ($\bar{1}10$) facets. MnAs layers grown on GaAs (110) are typically (1 $\bar{1}00$)-oriented with the orientation relationship MnAs[11 $\bar{2}0$] \parallel GaAs[1 $\bar{1}0$] and MnAs[0001] \parallel GaAs[001].² Therefore the c -axis in the MnAs shell is expected to tilt in the sidewall plane by an angle of 54.7° from the substrate normal, which is the angle between the [001] and [111] directions in the ($\bar{1}10$) plane.

As the magnetic hard axis of bulk MnAs is along the c -axis, the magnetic easy axis of the nanowires is expected to be parallel to the plane of the substrate surface. We have examined the dependence of magnetization of the nanowires on an external magnetic field using a superconducting quantum interference device (SQUID) magnetometer, Fig. 4(a). Here, the external field is applied normal to the substrate. The magnetization of the nanowires was obtained as the difference of that of the specimen before and after removal of nanowires. The hard-axis behavior confirms that the c -axis of MnAs is perpendicular to the substrate. Using the saturation

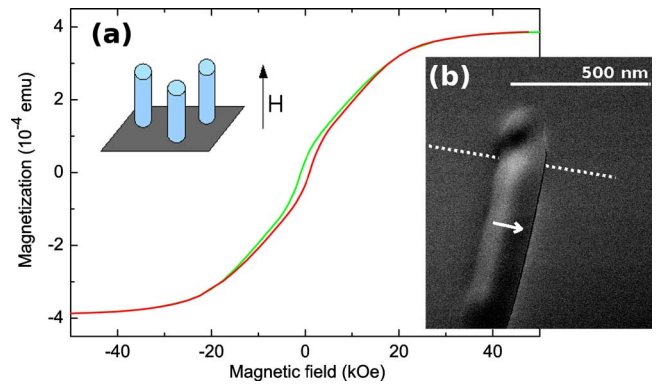


FIG. 4. (Color online) (a) Magnetization of sample A measured at a temperature of 10 K using a SQUID magnetometer. An external magnetic field H was applied normal to the substrate, as shown in the inset. The contribution of the substrate, including that of the MnAs layer on the substrate, has been subtracted. (b) Magnetic-force micrograph of a nanowire from sample C placed on a SiO₂/Si substrate. The location of the top of the GaAs core where the Au catalyst was present is indicated by the dotted line. The arrow indicates the direction of the magnetic moment in the middle section of the nanowire.

value in Fig. 4(a), the saturation magnetization is estimated to be 400–500 emu/cm³, which is reasonable for MnAs.²

In Fig. 4(b), we show a magnetic-force micrograph of an individual nanowire lying horizontally on a SiO₂/Si substrate. Here, the out-of-plane component of stray magnetic fields was measured. As indicated by the arrow, the direction of the magnetic moment, i.e., the magnetic easy axis, can be interpreted to be orthogonal to the nanowire axis, which is consistent with the c -axis orientation deduced above.

¹C. M. Lieber and Z. L. Wang, MRS Bull. **32**, 99 (2007).

²L. Däweritz, Rep. Prog. Phys. **69**, 2581 (2006).

³M. Ramsteiner, H. Y. Hao, A. Kawaharazuka, H. J. Zhu, M. Kästner, R. Hey, L. Däweritz, H. T. Grahn, and K. H. Ploog, Phys. Rev. B **66**, 081304 (2002).

⁴P. Landeros, O. J. Suarez, A. Cuchillo, and P. Vargas, Phys. Rev. B **79**, 024404 (2009).

⁵J. C. Harmand, G. Patriarche, N. Péré-Laperme, M.-N. Mérat-Combes, L. Travers, and F. Glas, Appl. Phys. Lett. **87**, 203101 (2005).

⁶V. Schmidt, P. C. McIntyre, and U. Gösele, Phys. Rev. B **77**, 235302 (2008).

⁷D. K. Satapathy, B. Jenichen, W. Braun, V. M. Kaganer, L. Däweritz, and K. H. Ploog, J. Phys. D **38**, A164 (2005).

⁸T. Suzuki and H. Ido, J. Phys. Soc. Jpn. **51**, 3149 (1982).

⁹Y. G. Tsui and T. W. Clyne, Thin Solid Films **306**, 23 (1997).

¹⁰Similar idea was independently presented in C. T. Foxon, S. V. Novikov, J. L. Hall, R. P. Campion, D. Cherns, I. Griffiths, and S. Khongphetsak, J. Cryst. Growth **311**, 3423 (2009).

¹¹This corresponds to the condition of nanowires covering the whole surface in the flux incidence direction: $(2r)(L \sin \varphi) = \rho^{-1}$.

¹²V. G. Dubrovskii, N. V. Sibirev, J. C. Harmand, and F. Glas, Phys. Rev. B **78**, 235301 (2008).

¹³The direct deposition explains the puzzle that nanowires can grow longer than the diffusion length.

¹⁴N. Begum, M. Piccin, F. Jabeen, G. Bais, S. Rubini, F. Martelli, and A. S. Bhatti, J. Appl. Phys. **104**, 104311 (2008).

¹⁵G. D. Mahan, R. Gupta, Q. Xiong, C. K. Adu, and P. C. Eklund, Phys. Rev. B **68**, 073402 (2003); D. Spirkoska, G. Abstreiter, and A. Fontcuberta i Morral, Nanotechnology **19**, 435704 (2008).

¹⁶D. G. Ramlan, S. J. May, J. Zheng, J. E. Allen, B. W. Wessels, and L. J. Lauhon, Nano Lett. **6**, 50 (2006).

¹⁷For our GaAs nanowires we have observed no evidence for the transition in the sidewall facet orientation during growth reported in M. C. Plante and R. R. LaPierre, J. Cryst. Growth **310**, 356 (2008).

¹⁸A. Trampert, Physica E (Amsterdam) **13**, 1119 (2002).

¹⁹A. Fontcuberta i Morral, D. Spirkoska, J. Arbiol, M. Heigoldt, J. R. Morante, and G. Abstreiter, Small **4**, 899 (2008).

²⁰M. I. McMahon and R. J. Nemes, Phys. Rev. Lett. **95**, 215505 (2005).